Title

Deletion of GLUT1 in mouse lens epithelium leads to cataract formation

Journal

Experimental Eye Research, 172(8)

ISSN

0014-4835

Authors

Swarup, Aditi
Bell, Brent A
Du, Jianhai
et al.

Publication Date

2018-07-01

DOI

10.1016/j.exer.2018.03.021

Peer reviewed

HHS Public Access

Author manuscript

Exp Eye Res. Author manuscript; available in PMC 2019 August 30.

Published in final edited form as:

Exp Eye Res. 2018 July ; 172: 45–53. doi:10.1016/j.exer.2018.03.021.

Deletion of GLUT1 in mouse lens epithelium leads to cataract formation.

Aditi Swarup[a], **Brent A. Bell**[b], **Jianhai Du**[c], **John Y. S. Han**[a], **Jamie Soto**[d,e], **E. Dale Abel**[d,e], **Arturo Bravo-Nuevo**[f], **Paul G. FitzGerald**[g], **Neal S. Peachey**[b,h,i], **Nancy J. Philp**[a,*]

[a]Department of Pathology, Anatomy & Cell Biology, Thomas Jefferson University, Philadelphia, PA

[b]Cole Eye Institute, Cleveland Clinic, Cleveland, OH

[c]West Virginia University Eye Institute, Morgantown, WV

[d]Fraternal Order of Eagles Diabetes Research Center, University of Iowa, Iowa City, IA

[e]Division of Endocrinology & Metabolism, Carver College of Medicine, University of Iowa, Iowa City, IA

[f]Department of Bio-Medical Sciences, Philadelphia College of Osteopathic Medicine, Philadelphia, PA

[g]Department of Cell Biology & Human Anatomy, University of California at Davis, Davis, CA

[h]Louis Stokes Cleveland VA Medical Center, Cleveland, OH

[i]Department of Ophthalmology, Cleveland Clinic Lerner College of Medicine of Case Western Reserve University, Cleveland OH

Abstract

The primary energy substrate of the lens is glucose and uptake of glucose from the aqueous humor is dependent on glucose transporters. GLUT1, the facilitated glucose transporter encoded by *Slc2a1* is expressed in the epithelium of bovine, human and rat lenses. In the current study, we examined the expression of GLUT1 in the mouse lens and determined its role in maintaining lens transparency by studying effects of postnatal deletion of *Slc2a1*. *In situ* hybridization and immunofluorescence labeling were used to determine the expression and subcellular distribution of GLUT1 in the lens. *Slc2a1* was knocked out of the lens epithelium by crossing transgenic mice expressing *Cre recombinase* under control of the GFAP promoter with $Slc2a1^{loxP/loxP}$ mice to generate $Slc2a1^{loxP/loxP}$;$GFAP\text{-}Cre^{+/0}$ (*LensΔGlut1*) mice. *LensΔGlut1* mice developed visible lens opacities by around 3 months of age, which corresponded temporally with the total loss of detectable GLUT1 expression in the lens. Spectral domain optical coherence tomography (SD-OCT) imaging was used to monitor the formation of cataracts over time. SD-OCT imaging revealed that small nuclear cataracts were first apparent in the lenses of *LensΔGlut1* mice

*Corresponding author: Dr. Nancy J. Philp, PhD, Department of Pathology Anatomy & Cell Biology, Thomas Jefferson University, 1020 Locust St, Philadelphia, PA 19107, Tel: 215-503-7854, Nancy.Philp@jefferson.edu.

beginning at about 2.7 months of age. Longitudinal SD-OCT imaging of *LensΔGlut1* mice revealed disruption of mature secondary fiber cells after 3 months of age. Histological sections of eyes from *LensΔGlut1* mice confirmed the disruption of the secondary fiber cells. The structural changes were most pronounced in fiber cells that had lost their organelles. In contrast, the histology of the lens epithelium in these mice appeared normal. Lactate and ATP were measured in lenses from *LensΔGlut1* and control mice at 2 and 3 months of age. At 2 months of age, when GLUT1 was still detectable in the lens epithelium, albeit at low levels, the amount of lactate and ATP were not significantly different from controls. However, in lenses isolated from 3-month-old *LensΔGlut1* mice, when GLUT1 was no longer detectable, levels of lactate and ATP were 50% lower than controls. Our findings demonstrate that *in vivo*, the transparency of mature lens fiber cells was dependent on glycolysis for ATP and the loss of GLUT1 transporters led to cataract formation. In contrast, lens epithelium and cortical fiber cells have mitochondria and could utilize other substrates to support their anabolic and catabolic needs.

Keywords

Slc2a1; Glut1; Lens; Cataract; Optical Coherence Tomography

1. Introduction:

Glucose is the primary energy substrate of many tissues including the avascular ocular lens. The uptake of glucose into cells is regulated by facilitated and sodium-coupled glucose transporters whose expression pattern and subcellular distribution vary in a developmental and tissue specific manner. Facilitated glucose transporters are encoded by the *Slc2* gene family and sodium-coupled glucose transporters are encoded by the *Slc5* gene family (Wood and Trayhurn, 2003). GLUT1, encoded by *Slc2a1*, is the major facilitative glucose transporter expressed in the eye (Kumagai et al., 1994)(Takata, 1996)(Merriman-Smith et al., 2003).

In mammals, the lens is derived from surface ectoderm and the adult lens is comprised of lens epithelium and lens fiber cells. In the equatorial region of the lens, epithelial cells proliferate then differentiate into elongated fiber cells. Differentiation into mature secondary fiber cells is accompanied by loss of organelles, including nuclei and mitochondria. The lens epithelium has mitochondria that can utilize oxidative phosphorylation for the generation of ATP, while the fully differentiated lens fiber cells are reliant on glycolytic metabolism of glucose to support their energy demands. In the lens, glucose uptake is mediated by glucose transporters, however across different species the specific transporters used and their localization differs (Merriman-Smith et al., 1999)(Merriman-Smith et al., 2003)(Mantych et al., 2015)(Lim et al., 2017). In bovine and human lenses, GLUT1 is the only glucose transporter expressed and is found throughout the lens including lens epithelium and fiber cells. The lens epithelium and fiber cells of the rat expressed GLUT1 while GLUT3, SGLT1 and SGLT2 were only expressed in fiber cells in the inner cortex and core regions (Lim et al., 2017).

The lens is an avascular tissue and relies on the aqueous humor for supply of oxygen and nutrients including glucose (Dahm et al., 2011). Within the lens, the lens epithelium has been identified as the more metabolically active compartment (Bhat, 2001). Previous studies have shown that in the presence of glucose, both the lens epithelium and fiber cells from freshly isolated rabbit lenses were able to maintain ATP levels under aerobic and anaerobic conditions. In the absence of glucose the rabbit lens epithelium and fiber cells rapidly lost ATP (Winkler and Riley, 1991). In another study, rat lenses were incubated *ex vivo* in decreasing concentrations of glucose, which resulted in decreased ATP and cataract formation when glucose fell below 2 mM. Cells were unable to maintain the osmotic gradient, leading to an increase in Na^+ and a decrease in K^+ levels in these lenses. (Chylack, 1975). The osmotic cataracts formed in these lenses *ex vivo* mimicked the cataracts *in vivo* and also mimicked hypoglycemic lamellar cataracts reported in children (Merin et al., 1971). In previous studies, glucose was the only substrate provided in the buffer and other metabolic fuels found in the aqueous humor such as amino acids and lipids were not tested to see if they could support ATP production in the lens epithelium.

In the present study, we characterized the expression of glucose transporters in the developing and adult mouse lens and showed that GLUT1 is the primary transporter expressed in the lens epithelium. We found that mice with a homozygous deletion of *Slc2a1* from the lens epithelium developed cataracts, which were not observed in heterozygous mice expressing a single GLUT1 allele. These studies thus establish a critical role of GLUT1 expression in the mouse lens epithelium for the maintenance of lens transparency.

2. Materials and Methods

2.1 Animals

Mice carrying a floxed *Slc2a1* allele (Winkler et al., 2015) were crossed to transgenic lines that expressed *Cre recombinase* under control of the promoter for glial fibrillary acidic protein (GFAP; Jax Stock #012886; (Garcia et al., 2004)) or the promoter for platelet derived growth factor receptor, alpha polypeptide (PDGFRa, Jax Stock #013148; (Roesch et al., 2008)). We used a two-generation cross to generate mice that were $Slc2a1^{loxP/loxP}$ homozygous and *Cre* transgenic, as well as controls. Animals were euthanized with an overdose of ketamine (100 mg/kg) and xylazine (10 mg/kg) and the eyes were enucleated for histological and immunohistochemical or biochemical analyses. All animal procedures were conducted with approval of the local Institutional Animal Care & Use Committees and conformed to the ARVO statement for use of animals in ophthalmic and vision research.

2.2 Spectral Domain Optical Coherence Tomography

Spectral domain optical coherence tomography (SD-OCT) imaging of mouse eyes was conducted at both Thomas Jefferson University and the Cleveland Clinic. At Thomas Jefferson University, mice were anesthetized with a mixture of ketamine (100 mg/kg) and xylazine (10 mg/kg), after which the pupils were dilated with eye drops (10% phenylephrine HCl ophthalmic solution, Akorn, Lake Forest, IL). A Bioptigen (Durham, NC) SD-OCT system imaged the eye at 840 nm using a 10 mm Telecentric lens to image the lenses. Lenses were imaged at 4 mm rectangular measurement of 1000 A-scans by 100 B-scans per image

and averaged over 25 images. Bioptigen InVivoVue software was used to average the images.

The procedures used for imaging the mouse eye at Cleveland Clinic have been published (Bell et al., 2014)(Bell et al., 2015). In brief, mice were anesthetized using sodium pentobarbital (68 mg/kg) and pupils dilated with 1 μl of 0.5% tropicamide/phenylephrine combination drops. Topical anesthesia was induced by a single application (~10 μl) of 0.5% proparacaine. A Bioptigen SD-OCT System (840HR, SDOIS) was used to image the anterior segment of the eye using a 25 mm telecentric lens. Orthogonal radial scans (1000 A-scans/B-scan by 15 frames) were collected through the horizontal and vertical meridian just below, and to the side, of the corneal apex reflex. The B-scans from each orientation were displayed as 1.5 mm (depth) × 5 mm (width) region of interest and exported to ImageJ (Schneider et al., 2012) for co-registration and averaging using the StackReg and TurboReg plugins (Thevenaz et al., 1998).

2.3 Immunofluorescence

Mouse eyes were fixed in cold (-80°C) methanol:acetic acid (97:3) as previously described (Sun et al., 2015). The fixed eyes were either processed for paraffin or optimal cutting temperature (OCT) compound embedding. Blocks processed for OCT were stored at -80°C. For both paraffin and OCT-embedded eyes, 10 μm sections were cut. Paraffin sections were deparaffinized using xylene and rehydrated in a graded series of ethanol then water. Frozen sections and paraffin sections were used for immunolocalization. Sections were blocked in 5% BSA in phosphate buffered saline (PBS) with 0.1% Tween (PBST) for 1 h then incubated in primary antibody diluted in 1% BSA in PBST overnight at 4°C. Sections were then incubated with Alexa Fluor 546 Donkey anti-Rabbit (A10040; ThermoFisher Scientific, Waltham, MA), 1:500) or Alexa Fluor 555 Goat anti Mouse (A21422; ThermoFisher Scientific, Waltham, MA), 1:500) for 1 h and with DAPI (4’6-Diamidino-2- Phenylindole, Dihydrochloride) for 5 min. Two anti-GLUT1 antibodies were used: (GT11-A (Alpha Diagnostics, San Antonio, Texas), 1:250; MA5–11315 (Thermo Fisher Scientific, Waltham, MA), 1:50). Both antibodies recognize the cytoplasmic tails of GLUT1, had the same distribution in the mouse lens, and yielded no signal in tissues lacking GLUT1. Paraffin embedded sections were also stained with hematoxylin and eosin (H&E) to examine the histological changes in lenses as previously described (Lee et al., 2014). Sections were imaged on LSM 780 NLO laser scanning microscope (Carl Zeiss, Oberkochen, Germany) using 63x/1.4 NA ApoPlan and 10x/0.3 NA EC NeoPlan objectives.

2.4 ATP and Lactate measurements

Isolated lenses were flash frozen in liquid nitrogen immediately after isolation from euthanized mice as described above. Tissue was homogenized with 1.5 ml pellet pestles (Kimble, 749521–1500) in ice cold 0.6N perchloric acid and centrifuged for 15 min at 15000g. Supernatants were collected and neutralized with 1.8M potassium carbonate then centrifuged for 15 min. The supernatants were used for lactate and ATP analyses. Both lactate and ATP were measured using available assay kit (lactate; Trinity Biotech (Jamestown, NY); Cat# 735–10), (ATP; Invitrogen (Carlsbad, CA); A220066) following manufacturer’s instructions.

2.5 *In situ* hybridization

After enucleation, eyes were embedded in OCT compound and immediately frozen in liquid nitrogen. Blocks were then stored at -80°C. Frozen sections were cut (10 μm) and placed on positively charged Diamond white glass microscope slides (Globe Scientific (Paramus, NJ) 1358W). RNAscope (Advanced Cell Diagnostics, Hayward, CA) was performed on these fresh frozen sections using probes for *Glut1* with the Manual Red Detection Kit 2.5 following manufacturer's instructions (Advanced Cell Diagnostics, Hayward, CA). Briefly, fresh frozen sections were fixed with 4% paraformaldehyde for 15 min at 4°C, dehydrated in ethanol and pretreated with hydrogen peroxide and Protease IV. Samples were individually incubated with RNAscope probes for *Slc2a1* (GLUT1) (Mm-Slc2a1 Cat No. 458671, Advanced Cell Diagnostics) for 2 h at 40°C. Preamp steps 1–6 were performed and RNAscope 2.5 HD Manual Detection Kit Red (Cat No. 322350) was used for visualizing the hybridization. The nuclear stain DAPI was applied for 5 min. The sections were imaged on a Nikon (Melville, NY) Eclipse E800 fluorescent microscope using the 10x/0.30 or 40x/0.75 Plan Fluor objectives.

2.6 Glucose measurement in the Aqueous Humor

Mice were anesthetized with ketamine (100 mg/kg) and xylazine (10 mg/kg). After 30 min, a small hole was made in the cornea using a 25G needle (BD PrecisionGlide Needle, BD-305124, Franklin Lakes, NJ) and aqueous humor was collected with a pipette (P20, Gilson). Glucose concentration was measured in 3 μl aqueous humor using a glucose meter (Precision Xtra Glucose meter; Abbott, Alameda, CA). Glucose was measured in tail vein blood from each mouse using the glucose meter.

Data was expressed as a ratio of glucose in the aqueous humor to blood glucose in control (n=7) and *LensΔGlut1* (n=8) mice.

2.7 Western Blot

Lenses were isolated and the epithelium was carefully separated from the fiber cells. The lens epithelium was homogenized in 50 μl RIPA (Radioimmunoprecipitation Assay, Thermo Scientific, Rockford, IL) with protease inhibitors and lens fiber cells were homogenized in 100 μl of RIPA with protease inhibitors and extracted on ice for 30 min. Samples were centrifuged for 30 min at 15,000g and the supernatants removed for protein determination and western blot analysis. Protein was measured using BCA reagent (Cat # 23225, Thermo Fisher Scientific, Rockford, IL). A total of 10 μg of lens epithelium protein and 10 μg of lens fiber protein was loaded on 4–12% NuPage Bis-Tris Protein gels (Invitrogen, NP0321BOX) and electrophoretically transferred onto Immobilon-P membrane (Millipore, Beford, MA). Membranes were incubated for 1 h at room temperature in blocking buffer (5% powdered milk in Tris buffered saline with 0.1% Tween20 (TBST)) then incubated overnight with GLUT1 (1:1000, Alpha Diagnostics GT11-A), GFAP (1:1000, Sigma SAB4300647) and ß-Catenin (1:5000, C-2206, Sigma) antibodies. Membranes were washed three times with TBST and incubated for an hour with Peroxidase Affinipure Goat Anti-Rabbit antibody (1:2000) (Jackson ImmunoResearch 111–035-144). Bands were detected using chemiluminescence (Supersignal West Dura, Thermo Fisher Scientific, Waltham, MA) on FluorChem M ProteinSimple (San Jose, CA) detection system.

2.8 Reverse Transcriptase-PCR

Whole lenses were isolated and homogenized in 1ml Trizol (Cat# 15596026, Thermo Fisher Scientific, Rockford, IL). RNA was extracted according to manufacturer specifications. 1μg of RNA was reverse transcribed to 20μl cDNA using EcoDry Premix ((oligo dT) Cat # 639543 Takara Bio USA, Mountain View, CA). PCR was performed using 0.5μl of cDNA. The PCR mix was heated to 95°C for 5 min to heat activate the Taq DNA polymerase. Amplification was performed for 30 cycles with 30s denaturation at 94°C, 30s annealing at 60°C and 45s elongation at 72°C. The PCR product was analyzed on a 1.5% agarose gel. Primers sequences are shown in Table 1.

2.9 Amino acids quantification by gas chromatography mass spectrometry (GC/MS)

Briefly, amino acids were extracted by mixing 2 μl of humor sample with 8 μl of cold methanol and 1 μl internal standard (Myristic acid-d27). The extracts were dried under vacuum and derivatized by methoxyamine and N-tertbutyldimethylsilyl-N-methyltrifluoroacetamide as described in detail (Du et al., 2015)(Chao et al., 2017). An Agilent 7890B/5977B GC/MS system with an Agilent DB-5MS column (30 m × 0.25 mm × 0.25 μm film) was used for GC separation and analysis of metabolites. Ultra–high-purity helium was the carrier gas at a constant flow rate of 1 mL/min. One microliter of sample was injected in split-less mode by the auto sampler. The temperature gradient started at 95 °C with a hold time of 2 min and then increased at a rate of 10 °C/min to 300 °C, where it was held for 6 min. The temperatures were set as follows: inlet 250 °C, transfer line 280 °C, ion source 230 °C, and quadrupole 150 °C. Mass spectra were collected from m/z 80–600 under selective ion monitoring mode. The data was analyzed by Agilent MassHunter Quantitative Analysis Software.

3. RESULTS

3.1 Slc2a1 is the most highly expressed glucose transporter in the mouse lens

To determine which glucose transporters were expressed in the mouse lens we analyzed single cell microarray data from GEO datasets of whole mouse lens (GSE99218), mouse lens epithelium (GSE13402) and compared it with microarray data from rat (GSE50604) lenses (Greiling et al., 2009)(Wolf et al., 2013). *Slc2a1* (GLUT1) was found to be the primary glucose transporter expressed in the mouse lens (data not shown). In Fig. 1A, we confirmed the microarray data using RT-PCR comparing different glucose transporters in WT whole mouse lens, retina, muscle and kidney. *Slc2a1* was the only glucose transporter expressed at detectable levels in the lens. *In situ* hybridization with the *Slc2a1* (GLUT1) probe showed that the mRNA was expressed throughout the lens epithelium from the anterior epithelium (Fig. 1Ba) to the equatorial region and there was some signal in the differentiating fiber cells but no signal was detected in mature lens fiber cells (Fig. 1Bb). Immunofluorescence localization was used to determine the distribution of GLUT1 in the developing and adult lens. GLUT1 was detected throughout the lens epithelium at embryonic day 15 and was detected at lower levels in the primary fiber cells (Fig. 1Ca, a'). In the postnatal mouse lens, GLUT1 was primarily polarized to the basolateral membrane of the lens epithelium including in the equatorial region (Fig. 1Cb,b',c,c'). There was some GLUT1 expression detected in the apical lens epithelium which could contribute to

transepithelial transport of glucose to the fiber cells. Overexposure of the images in Fig. 1Ca'b'c' showed there was no GLUT1 expression detected in the mature fiber cells of 3 week (Fig. 1Cb'') and 3-month-old WT lenses (Fig. 1Cc'') with only a small amount of GLUT1 expression in the differentiating fiber cells around the equatorial region. As noted in Methods, we used two different GLUT1 antibodies against different C-terminal epitopes and derived from rabbit (Alpha diagnostics) or mouse (Thermo Fisher). The images shown in Figure 1C and Figure 2B,D were made using the Alpha Diagnostics antibody, but the Thermo Fisher antibody yielded similar results (data not shown).

In vitro studies showed that glucose was essential for maintaining lens transparency. To examine whether this was the case *in vivo*, where other carbon fuels are available, we crossed *Slc2a1*$^{loxP/loxP}$ and *GFAP-Cre*$^{+/0}$ transgenic mice. While GFAP-Cre is often used to target retinal Müller glial cells (Duan et al., 2014), GFAP is also expressed in the lens epithelium of some strains of mice as early as E18 (Boyer et al., 1990) (Hatfield et al., 1985), suggesting *Slc2a1* could be conditionally knocked out of lens epithelium using this approach. Our mating scheme generated *Slc2a1*$^{loxP/loxP}$*; GFAP-Cre*$^{+/0}$ mice (hereafter *LensΔGlut1*) and control animals (results from *Slc2a1*$^{loxP/loxP}$ non-transgenic or *GFAP-Cre* $^{+/0}$ mice were not distinguishable from C57BL6-J WT mice).

The expression of *Slc2a1* in the *LensΔGlut1* was examined using *in situ* hybridization. *Slc2a1* was not detected in lenses from 3-month-old *LensΔGlut1* mice, neither in the anterior (Fig. 2Aa) nor the equatorial epithelium (Fig. 2Ab) confirming our knockout. *Slc2a1* was detected in the ciliary epithelium of *LensΔGlut1* mice, indicating that the transport of glucose into the aqueous humor would not be compromised in the *LensΔGlut1* model (Fig. 2Ab). GLUT1 expression was detected by immunofluorescence in the equatorial lens epithelium in 1 month (Fig. 2Ba) and 2-month-old *LensΔGlut1* mice (Fig. 2Bb), albeit at very low levels. The GLUT1 was still detectable presumably because the GFAP-Cre was not expressed until E18, and GLUT1 was not rapidly turned over. GLUT1 expression was not detected in western blots of lysates of lens epithelium prepared from 3-month-old *LensΔGlut1* mice (Fig. 2C). Immunolocalization of GLUT1 in sections of lenses from 3-month-old *LensΔGlut1* mice confirmed the loss of expression of GLUT1 (Fig. 2D).

3.2 Loss of GLUT1 expression leads to cataract formation

The *LensΔGlut1* mice developed lens opacities that were visible by eye beginning at 3 months, an age which corresponded to the disappearance of GLUT1 from the lens epithelium (Fig 3Aa). The eyes were imaged using SD-OCT and the white opacity observed in Fig. 3Aa' (arrowhead) is due to the increased reflectivity of the cataract. Cataracts were not detected by SD-OCT in 5-month old heterozygous (*Slc2a1*$^{loxP/+}$*; GFAP-Cre*$^{+/0}$ (*LensΔGlut1Het*) mice carrying a single *Slc2a1* allele, as shown in Fig 3Ab'. Western blots comparing GLUT1 expression levels in control lens epithelium with *LensΔGlut1Het* lens epithelium showed GLUT1 level in the heterozygous lens epithelium was approximately half of the control. The findings with the *LensΔGlut1Het* mice demonstrate that neither Cre expression nor haploinsufficiency of GLUT1 leads to cataract formation in heterozygous mice.

The development of the cataract was followed over time in individual *LensΔGlut1* mice using SD-OCT imaging. As shown in Fig. 4A, the lens of a control mouse looks normal by SD-OCT even at 7 months of age. In comparison, a nuclear cataract was beginning to form in a 2.7-month-old *LensΔGlut1* animal (arrowhead) (Fig. 4B). This cataract became progressively more severe as the mouse aged (Fig.4C,D). To confirm the time line of appearance of these cataracts, we performed longitudinal SD-OCT on seven *LensΔGlut1* mice at weekly intervals, and found a similar pattern of cataract formation where a nuclear cataract was observed by day 85 which became a white cataract around day 100.

Histological changes in the lens were visualized by H&E staining of lens sections from *LensΔGlut1* at ages that bracketed the onset of cataract formation (Fig. 4E–J). Prior to 3 months of age (Fig. 4F), the morphology of *LensΔGlut1* lenses appeared normal (Fig. 4E). The disruption of the nuclear region of the lens seen in Fig. 4E,F,G was an artifact of tissue preparation. The morphology of the lens epithelium in *LensΔGlut1* mice appeared normal even at 5 months of age. There was no cell death based on TUNEL analysis (data not shown) although dysplastic epithelia were observed in some eyes (data not shown). Initially, the lens fiber cells in *LensΔGlut1* mice elongated and differentiated normally (Fig. 4F). After 3 months of age, *LensΔGlut1* mice showed disruption of secondary lens fiber cells that had lost their organelles (Fig. 4G and H). Higher magnification images of the micrograph shown in Fig 4H demonstrate vacuolization and disorganization of lens fiber cells occurs after the loss of organelles (Fig. 4I,J). The abrupt disorganization of mature lens fiber cells that have lost their organelles is evident in Fig. 4I.

GFAP is also expressed in retinal Müller glial cells (Duan et al., 2014). To control for the possibility that the phenotype might reflect deletion of GLUT1 from Müller glial cells, we also crossed the *Slc2a1*$^{loxP/loxP}$ line to *PDGFRa-Cre*$^{+/0}$ transgenic mice, as the *PDGFRa-Cre*$^{+/0}$ is expressed in Müller glial cells (Roesch et al., 2008). The lenses of 7-month old *Slc2a1*$^{loxP/loxP}$*; PDGFRa-Cre*$^{+/0}$ mice looked clear by SD-OCT (data not shown).

3.3 In the absence of GLUT1, no other glucose transporter is upregulated

To determine whether any other glucose transporters were upregulated in the absence of GLUT1, we performed RT-PCR on 2-month and 4-month-old control and *LensΔGlut1* whole lens comparing *Slc2* and *Slc5* glucose transporters. Brain and kidney were used as positive controls and RPLP0 was used as loading control (Fig. 5). There was no GLUT1 mRNA detected in *LensΔGlut1* lenses as well as, no upregulation of other glucose transporters such as GLUT3, SGLT1 and SGLT2. *Slc2a12* mRNA was slightly increased in the *LensΔGlut1* but there was not a validated GLUT12 antibody to look at protein expression. The fact that mature fiber cells become vacuolated and disorganized in lenses of *LensΔGlut1* demonstrates that there is not another transporter compensating for the loss of *Slc2a1*.

3.4 GLUT1 is essential to support glycolysis and ATP production in the lens.

A number of *ex vivo* studies with isolated lenses have demonstrated the importance of glucose for generating ATP. Decreasing glucose levels resulted in a decrease in ATP, an increase in intracellular Na^+ and a decrease in intracellular K^+ resulting in cataract formation

(Chylack, 1975)(Winkler and Riley, 1991). To evaluate whether cataract formation in the *LensΔGlut1* mice was due to a decrease in glucose transport into the lens we measured the glucose concentrations of the aqueous humor and the blood in *LensΔGlut1* and in age-matched control mice. In control mice, glucose levels in the aqueous humor matched those in blood (Fig. 6A). In comparison, *LensΔGlut1* mice had blood glucose levels that matched those of controls, but had elevated glucose levels in the aqueous humor, consistent with decreased transport from the humor into the lens epithelial cells (Fig. 6A).

To determine whether loss of expression of GLUT1 in the lens epithelium led to reduced glycolysis and ATP, we measured ATP and lactate levels in lenses of *LensΔGlut1* and control mice. At 2 months of age, prior to cataract formation, when GLUT1 expression was low but detectable, there was no difference between *LensΔGlut1* and control mice with respect to lactate (Fig. 6B), and ATP (Fig. 6C) levels. At 3 months of age, when mice had developed cataracts, lactate levels reduced by 66.8% (Fig. 6B) and ATP levels were reduced by 55.7% (Fig. 6C) in lenses from *LensΔGlut1* mice compared to age matched controls.

4. Discussion

Previous studies performed on isolated lenses established an essential role for glycolysis in generating ATP required to maintain osmotic gradients and lens transparency (Winkler and Riley, 1991)(Chylack, 1975). In these *ex vivo* studies glucose was the only carbon source provided in the incubation media. In the present study, we demonstrated in an *in vivo* mouse model that glucose uptake by GLUT1 is required for maintaining metabolic homeostasis and transparency in the lens even when other metabolic substrates are available.

In the mature mouse lens, we found by immunofluorescence localization and immunoblot analysis that GLUT1 was most highly expressed in the basolateral membrane of the lens epithelium, which is bathed in the nutrient rich aqueous humor. Low levels of expression were detected in the fiber cells in the cortical region when images were overexposed (Fig. 1). These results are consistent with mouse lens proteome data showing that GLUT1 comprises only 1 % of the membrane protein in the fiber cells (Bassnett et al., 2009). During lens development, hyaloid vessels surround the growing lens providing a supply of nutrients and GLUT1 was detected in the primary fiber cells to facilitate glucose uptake. However, as the lens grows in size, the hyaloid vessels regress and ciliary epithelium transports glucose into the aqueous humor to support lens metabolism (Yoshioka, 1999). As GLUT1 was only detected at very low levels in the apical membrane of the mouse lens epithelium, glucose may diffuse into lens fiber cells via gap junctions (Goodenough et al., 1980). A similar system has been described for movement of glucose between pigmented and non-pigmented epithelium in the ciliary body and at the interface of maternal-fetal circulation (Kumagai, 1999). The flow of glucose from the lens epithelium to lens fiber cells is essential since, like red blood cells, lens fiber cells lose their organelles as they mature and rely solely on glycolysis for ATP production (Winkler and Riley, 1991). In contrast, the lens epithelium and fiber cells in the outer cortex have mitochondria and can oxidize other substrates to support their anabolic and catabolic needs (Kinoshita, 1965). The distribution of glucose transporters in the mouse lens differs from that observed in larger lenses including rat, bovine, and human lenses where GLUT1 or GLUT3 are both detected in fiber cells(Lim et

al., 2017). In these larger lenses the observed expression of glucose transporters in differentiating and mature fiber cells suggests glucose diffuses through the extracellular space and that fiber cells directly uptake the glucose delivered to them via the extracellular space.

To determine the importance of GLUT1 in maintaining metabolic homeostasis and transparency in the lens, we used a genetic approach to delete *Slc2a1.* GLUT1$^{f/f}$ mice were crossed with GFAP-Cre mice to generate *LensΔGlut1het* and *LensΔGlut1* mouse lines. GFAP is expressed in the lens epithelium at E18 so the early development of the lens was not affected. The *LensΔGlut1het* mice did not develop cataracts even though the levels of GLUT1 expression were significantly reduced. This is consistent with the observation that patients with GLUT1 deficiency syndrome do not generally develop cataracts (Winkler et al., 2015). *LensΔGlut1* mice do not develop cataracts until about three months of age. The late onset of cataract formation in the *LensΔGlut1* mice correlates with the time required for complete loss of GLUT1 mRNA and protein. While GLUT1 expression levels were much lower in the 2-month-old *LensΔGlut1* mice relative to controls, it was adequate to maintain glycolysis and generate sufficient ATP to maintain transparency. At 3 months of age, when GLUT1 was no longer detectable, the levels of lactate and ATP were decreased compared to control mice. Mature fiber cells in the organelle free zone became vacuolated and disorganized while the lens epithelium and fiber cells that still had organelles retained their structural integrity. Lenses of the *LensΔGlut1* mice continued to grow in size demonstrating that glucose was not required for proliferation and differentiation into lens fiber cells. This suggests that other carbon sources can be used to support anabolic and catabolic processes in the lens epithelium and cortical fiber cells. Consistent with this observation, we found that while glucose was increased in the aqueous humor of *LensΔGlut1* mice compared to controls, the levels of several amino acids were decreased. The decrease in amino acids in the aqueous humor of the *LensΔGlut1* mice compared to the controls, suggests an increase in oxidation of amino acids may be used to support the metabolic needs of the epithelium and differentiating fiber cells in mice (Waley, 1964)(Trayhurn and Van Heyningen, 1973).

ATP is essential for maintaining the ionic balance of the lens (Michael and Bron, 2011). Without sufficient ATP there is an ionic imbalance due to Na^+K^+ATPase dysfunction. Previous studies have shown that rabbit lenses incubated *ex vivo* without glucose rapidly lost ATP in their lens epithelium and fiber cells (Winkler and Riley, 1991). In human patients, a deficiency of GLUT1 in erythrocytes leads to leakage of monovalent cations through the red blood cell membrane, resulting in osmotic instability and hemolysis (Bawazir et al., 2012) (Shibata et al., 2017). In the mouse lens epithelium, a decrease in GLUT1 led to a decrease in lactate and ATP production. The decrease in ATP would lead to disruption of the ionic balance of the lens due to water entry, causing cataracts similar to osmotic cataracts observed in previous studies (Auricchio and Libondi, 1983) (Bender, 1994).

The use of SD-OCT proved to be a reliable and non-invasive method of investigating the longitudinal development of cataracts in mice. The SD-OCT images of the *LensΔGlut1* lens mirrored what was noted on histological analysis. Only a small number of studies have used SD-OCT to image cataracts in humans (Ortiz et al., 2013)(Mansouri et al., 2014) and, to our knowledge, none have been conducted using mice. SD-OCT has many advantages over

histology including the ability to conduct longitudinal studies on animals as well as the elimination of tissue artifacts from fixation and processing tissue sections.

In summary, our studies provide new insight into the metabolism of the lens by using a genetic approach to delete *Slc2a1* from the mouse lens. We showed that mature lens fiber cells are dependent on glycolysis to maintain their metabolic needs and structural integrity while lens epithelium and differentiating fiber cells can oxidize other substrates. Our results show that changes in expression levels of metabolic transporters can contribute to cataract formation.

Supplementary Material

Refer to Web version on PubMed Central for supplementary material.

Acknowledgements:

Supported by grants from the National Eye Institute (R01 EY012042, P30 EY025585, R01 EY024549, P30 EY012576), the National Heart Lung and Blood Institute (HL087947), the Department of Veterans Affairs (I01 BX002340, Research Career Scientist) and an unrestricted grant from Research to Prevent Blindness to Department of Ophthalmology, Cleveland Clinic Lerner College of Medicine of Case Western Reserve University.

Abbreviations:

LensΔGlut1	$Slc2a1^{loxP/loxP}$; $GFAP\text{-}Cre^{+/0}$
LensΔGlut1Het	$Slc2a1^{loxP/+}$; $GFAP\text{-}Cre^{+/0}$
SD-OCT	Optical Coherence Tomography

References

Auricchio G, Libondi T, 1983 The physiologic and pharmacologic factors protecting the lens transparency and the update approach to the prevention of experimental cataracts: a review. Metab. Pediatr. Syst. Ophthalmol 7, 115–124. [PubMed: 6361446]

Bassnett S, Wilmarth PA, David LL, 2009 The membrane proteome of the mouse lens fiber cell. Mol. Vis 15, 2448–63. [PubMed: 19956408]

Bawazir WM, Gevers EF, Flatt JF, Ang AL, Jacobs B, Oren C, Grunewald S, Dattani M, Bruce LJ, Stewart GW, 2012 An infant with pseudohyperkalemia, hemolysis, and seizures: Cation-leaky GLUT1-deficiency syndrome due to a SLC2A1 mutation. J. Clin. Endocrinol. Metab 97, 987–993. [PubMed: 22170711]

Bell BA, Kaul C, Bonilha VL, Rayborn ME, Shadrach K, Hollyfield JG, 2015 The BALB/c mouse: Effect of standard vivarium lighting on retinal pathology during aging. Exp. Eye Res 135, 192–205. [PubMed: 25895728]

Bell BA, Kaul C, Hollyfield JG, 2014 A protective eye shield for prevention of media opacities during small animal ocular imaging. Exp. Eye Res 127, 280–287. [PubMed: 25245081]

Bender CJ, 1994 A hypothetical mechanism for toxic cataract due to oxidative damage to the lens epithelial membrane. Med. Hypotheses 43, 307–311. [PubMed: 7877524]

Bhat SP, 2001 The ocular lens epithelium. Biosci. Rep 21, 537–563. [PubMed: 11900326]

Boyer S, Maunoury R, Gomes D, de Nechaud B, Hill AM, Dupouey P, 1990 Expression of glial fibrillary acidic protein and vimentin in mouse lens epithelial cells during development in vivo and during proliferation and differentiation in vitro: comparison with the developmental appearance of GFAP in the mouse central nervous s. J Neurosci Res 27, 55–64. [PubMed: 2254956]

Chao JR, Knight K, Engel AL, Jankowski C, Wang Y, Manson MA, Gu H, Djukovic D, Raftery D, Hurley JB, Du J, 2017 Human retinal pigment epithelial cells prefer proline as a nutrient and transport metabolic intermediates to the retinal side. J. Biol. Chem 292, 12895–12905. [PubMed: 28615447]

Chylack LT, 1975 Mechanism of" hypoglycemic" cataract formation in the rat lens. I. The role of hexokinase instability. Invest. Ophthalmol. Vis. Sci 14, 746–755.

Dahm R, Van Marle J, Quinlan RA, Prescott AR, Vrensen GFJM, 2011 Homeostasis in the vertebrate lens: mechanisms of solute exchange. Phil. Trans. R. Soc. B 366, 1265–1277. [PubMed: 21402585]

Du J, Linton JD, Hurley JB, 2015 Probing Metabolism in the Intact Retina Using Stable Isotope Tracers. Metab. Anal. Using Stable Isot 561, 149–170.

Duan LJ, Takeda K, Fong GH, 2014 Hypoxia inducible factor-2a regulates the development of retinal astrocytic network by maintaining adequate supply of astrocyte progenitors. PLoS One 9, 1–31.

Garcia ADR, Doan NB, Imura T, Bush TG, Sofroniew MV, 2004 GFAP-expressing progenitors are the principal source of constitutive neurogenesis in adult mouse forebrain. Nat. Neurosci 7, 1233–1241. [PubMed: 15494728]

Goodenough DA, J.S.B.D. Ii, Lyons JE, 1980 Lens Metabolic Cooperation : A Study of Mouse Lens Transport and Permeability Visualized with Freeze-Substitution Autoradiography and Electron Microscopy. J. Cell Biol 86, 576–589. [PubMed: 6772650]

Greiling TMS, Stone B, Clark JI, 2009 Absence of SPARC leads to impaired lens circulation. Exp. Eye Res. 89, 416–425. [PubMed: 19401199]

Hatfield JS, Skoff RP, Maisel H, Eng L, Bigner DD, 1985 The lens epithelium contains glial fibrillary acidic protein (GFAP). J. Neuroimmunol 8, 347–57. [PubMed: 3891782]

Kinoshita JH, 1965 Pathways of glucose metabolism in the lens. Invest Ophthalmol Vis Sci 4, 619–628.

Kumagai AK, 1999 Glucose transport in brain and retina: implications in the management and complications of diabetes. Diabetes. Metab. Res. Rev 15, 261–73. [PubMed: 10495475]

Kumagai AK, Glasgow BJ, Pardridge WM, 1994 GLUT1 glucose transporter expression in the diabetic and nondiabetic human eye. Invest. Ophthalmol. Vis. Sci 35, 2887–94. [PubMed: 8188484]

Lee EK, Kim YJ, Kim JY, Song HB, Yu HG, 2014 Melissa officinalis extract inhibits laser-induced choroidal neovascularization in a rat model. PLoS One 9, 1–11.

Lim, Perwick RD, Li B, Donaldson PJ, 2017 Comparison of the expression and spatial localization of glucose transporters in the rat, bovine and human lens. Exp. Eye Res 161, 193–204. [PubMed: 28625822]

Mansouri M, Ramezani F, Moghimi S, Tabatabaie A, Abdi F, He M, Lin SC, 2014 Anterior segment optical coherence tomography parameters in phacomorphic angle closure and mature cataracts. Investig. Ophthalmol. Vis. Sci 55, 7403–7409. [PubMed: 25335976]

Mantych GJ, Hageman GS, Devaskar SU, 2015 Characterization Adult and Developing Isoforms. Endocrinology 133, 600–607.

Merin S, Crawford JS, Scheie HG, Rubenstein RA, A.D., Gabilan JC, C.J., AJ M, O'Connor CF, Crawford JD, Cohen JM, et al, Fraser GR, F.A., D H, WA W, Battaglia FC, LO L, RA M, H D, De Loore L, V.G.H., Etheridge JE Jr, M.J., Knobloch H, Sotos JF, Sherard ES, et al, Colle E, U.R., 1971 Hypoglycemia and Infantile Cataract. Arch. Ophthalmol 86, 495–498. [PubMed: 5165486]

Merriman-Smith BR, Krushinsky A, Kistler J, Donaldson PJ, 2003 Expression patterns for glucose transporters GLUT1 and GLUT3 in the normal rat lens and in models of diabetic cataract. Investig. Ophthalmol. Vis. Sci 44, 3458–3466. [PubMed: 12882795]

Merriman-Smith R, Donaldson P, Kistler J, 1999 Differential expression of facilitative glucose transporters GLUT1 and GLUT3 in the lens. Investig. Ophthalmol. Vis. Sci 40, 3224–3230. [PubMed: 10586946]

Michael R, Bron AJ, 2011 The ageing lens and cataract: a model of normal and pathological ageing. Phil. Trans. R. Soc. B 1278–1292. [PubMed: 21402586]

Ortiz S, Pérez-Merino P, Durán S, Velasco-Ocana M, Birkenfeld J, de Castro A, Jiménez-Alfaro I, Marcos S, 2013 Full OCT anterior segment biometry: an application in cataract surgery. Biomed. Opt. Express 4, 387–96. [PubMed: 23503926]

Roesch K, Jadhav AP, Trimarchi JM, Stadler MB, Roska B, Sun BB, Cepko CL, 2008 The Transcriptome of Retinal Mü ller Glial Cells. J. Comp. Neurol 509, 225–238. [PubMed: 18465787]

Schneider C. a, Rasband WS, Eliceiri KW, 2012 NIH Image to ImageJ: 25 years of image analysis. Nat. Methods 9, 671–675. [PubMed: 22930834]

Shibata T, Kobayashi K, Yoshinaga H, Ono H, Shinpo M, Kagitani-Shimono K, 2017 Another Case of Glucose Transporter 1 Deficiency Syndrome with Periventricular Calcification, Cataracts, Hemolysis, and Pseudohyperkalemia. Neuropediatrics, 390–393. [PubMed: 28582795]

Sun N, Shibata B, Hess JF, Fitzgerald PG, 2015 An alternative means of retaining ocular structure and improving immunoreactivity for light microscopy studies. Mol. Vis

Takata K, 1996 Glucose transporters in the transepithelial transport of glucose. J. Electron Microsc. (Tokyo). 45, 275–84. [PubMed: 8888584]

Thevenaz P, Ruttimann UE, Unser M, 1998 A pyramid approach to subpixel registration based on intensity. IEEE Trans. Image Process 7, 27–41. [PubMed: 18267377]

Trayhurn P, Van Heyningen R, 1973 The metabolism of glutamine in the bovine lens: Glutamine as a source of glutamate. Exp. Eye Res. 17, 149–154. [PubMed: 4759531]

Waley, 1964 Metabolism of amino acids in the lens. Biochem. J 91, 576–83. [PubMed: 5840719]

Winkler BS, Riley MV, 1991 Relative contributions of epithelial cells and fibers to rabbit lens ATP content and glycolysis. Investig. Ophthalmol. Vis. Sci 32, 2593–2598. [PubMed: 1869412]

Winkler EA, Nishida Y, Sagare AP, Rege SV, Bell RD, Perlmutter D, Sengillo JD, Hillman S, Kong P, Nelson AR, Sullivan JS, Zhao Z, Meiselman HJ, Wenby RB, Soto J, Dale Abel E, Makshanoff J, Zuniga E, De Vivo DC, Zlokovic BV, 2015 GLUT1 reductions exacerbate Alzheimer's disease vasculo-neuronal dysfunction and degeneration. Nat. Neurosci 18, 521–529. [PubMed: 25730668]

Wolf L, Gao CS, Gueta K, Xie Q, Chevallier T, Podduturi NR, Sun J, Conte I, Zelenka PS, Ashery-Padan R, Zavadil J, Cvekl A, 2013 Identification and Characterization of FGF2-Dependent mRNA: microRNA Networks During Lens Fiber Cell Differentiation. G3 Genes|Genomes| Genetics 3, 2239–2255. [PubMed: 24142921]

Wood IS, Trayhurn P, 2003 Glucose transporters (GLUT and SGLT): expanded families of sugar transport proteins. Br. J. Nutr 89, 3–9. [PubMed: 12568659]

Yoshioka M, 1999 Regression of the hyaloid vessels and pupillary membrane of the mouse. Anat Embryol 2004, 403–411.

Highlights:

- GLUT1 is the primary glucose transporter expressed in the mouse lens epithelium
- Deletion of GLUT1 from the lens epithelium leads to formation of cataracts in mouse lens at the age of approximately 3 months
- Cataract formation is accompanied by a decrease in ATP and lactate levels at 3 months
- Optical Coherence Tomography provides a useful tool for imaging cataract formation.

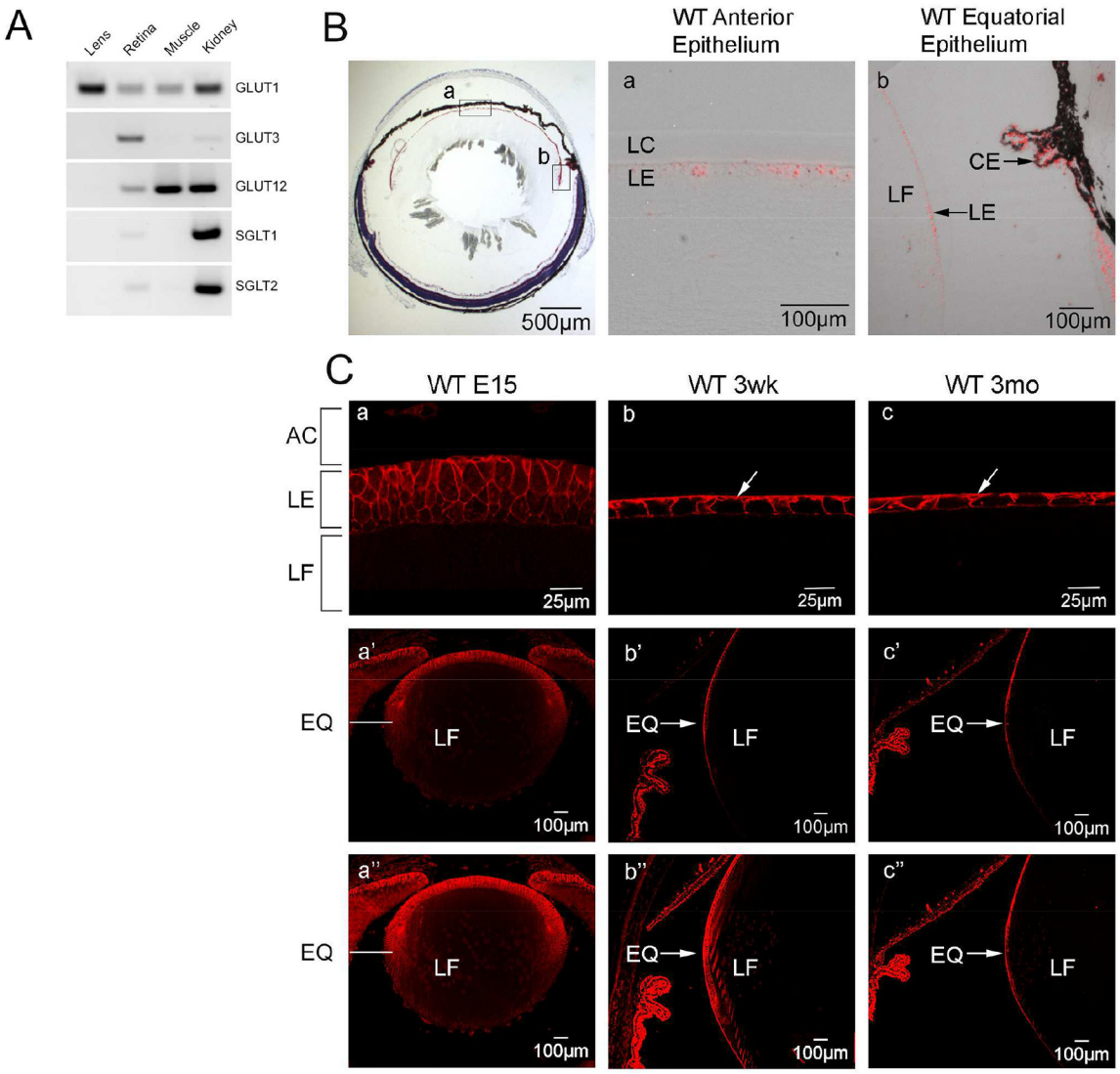

Figure 1: *Slc2a1* (GLUT1) is the most highly expressed transporter in mouse lens and is localized to the lens epithelium.

A: RT-PCR comparing expression of *Slc2* and *Slc5* glucose transporters in whole mouse lens, mouse retina, mouse muscle and mouse kidney. Reverse images of sybrgreen-stained amplicons after 30 cycles of PCR amplification. **B.** Expression of *Slc2a1* in WT mouse lens epithelium using *in situ* hybridization. Panels **a** and **b**, respectively, show *Slc2a1* transcript was detected (red) in anterior (a) and equatorial (b) lens epithelium. **C.** Immunolabeling with GLUT1 antibody at embryonic day 15 (E15) (a, a'), 3 weeks (b, b') and 3 months (c, c'). At E15 GLUT1 was detected throughout the lens including primary fiber cells. At later ages, GLUT1 was restricted to the basolateral membrane of the lens epithelium (arrows in b,c). Arrow in c' indicates GLUT1 expression in the epithelium in the equatorial region which was diminished towards the posterior region of the lens. AC: Anterior chamber, LC: Lens capsule, LE: Lens epithelium, LF: Lens fiber cells, EQ: Equatorial region, CE: Ciliary epithelium

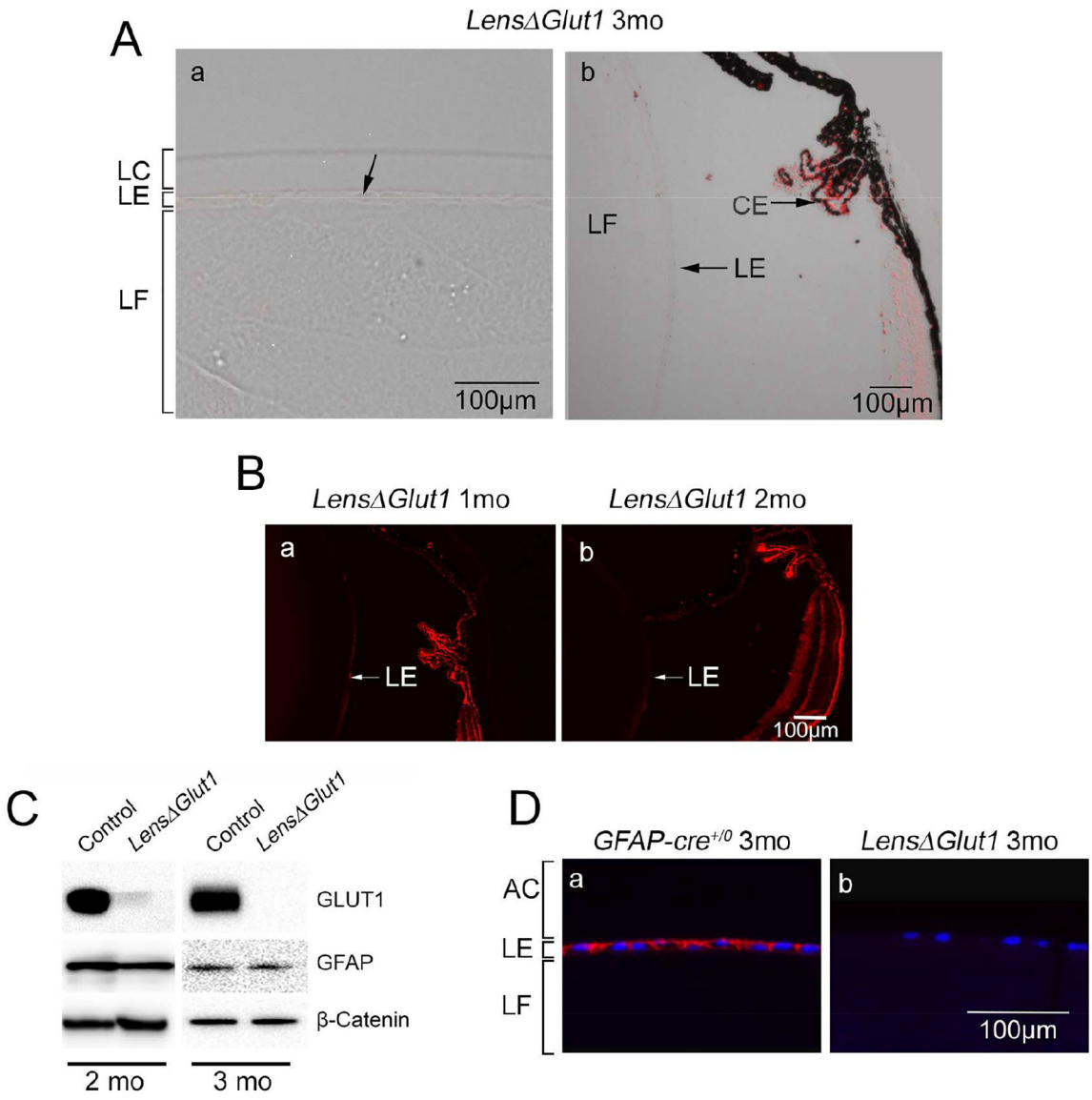

Figure 2: GLUT1 is deleted from *LensΔGlut1* lens

A. In the *LensΔGlut1* lens, *Slc2a1* expression was not detected in anterior (a) or equatorial (b) regions of the lens epithelium. In comparison, GLUT1 expression was retained in the ciliary epithelium. **B.** Immunofluorescence with GLUT1 in 1-month-old (a) and 2-month-old *LensΔGlut1* lenses (b). The GLUT1 levels were low in the 1-month-old *LensΔGlut1* mice and barely detectable in the 2-month-old mice. **C.** Western blot for GLUT1 in lysates of isolated lens epithelium from control and *LensΔGlut1* mice at 2 months (left) and 3 months (right) of age. Note that the residual expression of GLUT1 in the 2-month-old *LensΔGlut1* mouse is lost by 3 months of age. GFAP expression is unchanged in control versus *LensΔGlut1* mice. ß-Catenin was used as a loading control. **D.** Immunohistochemistry for GLUT1 in lens epithelium of 3-month-old control (a) and *LensΔGlut1* (b) mice. LC: lens capsule, LE: lens epithelium, LF: lens fiber cells, AC: Anterior chamber.

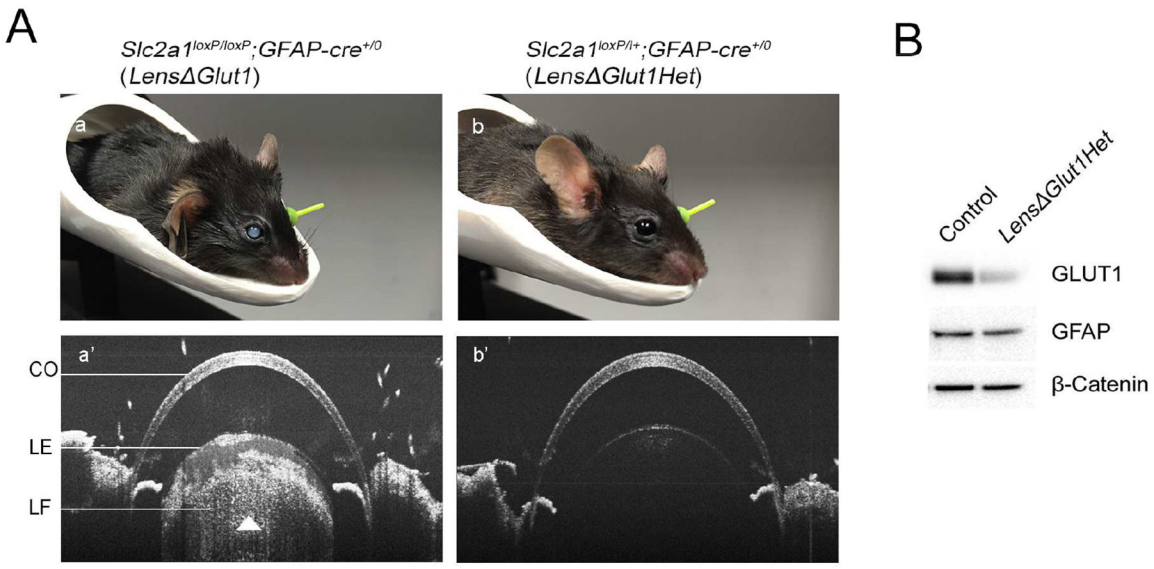

Figure 3: Formation of cataracts in *LensΔGlut1* mice

A. Images of 3-month-old *LensΔGlut1* (a,a') and 5-month-old *LensΔGlut1Het* (b,b') demonstrate presence of cataracts in 3-month-old *LensΔGlut1* mice but not in 5-month-old *LensΔGlut1Het* mice. In the SD-OCT image, the opacity is observed as hyper reflectivity which was observed in the *LensΔGlut1* (Aa') but not in the *LensΔGlut1Het* (Ab') **B.** Western blot of lysates from lens epithelium of control and *LensΔGlut1Het* mice. CO: Cornea, LE: Lens epithelium, LF: Lens fiber cells.

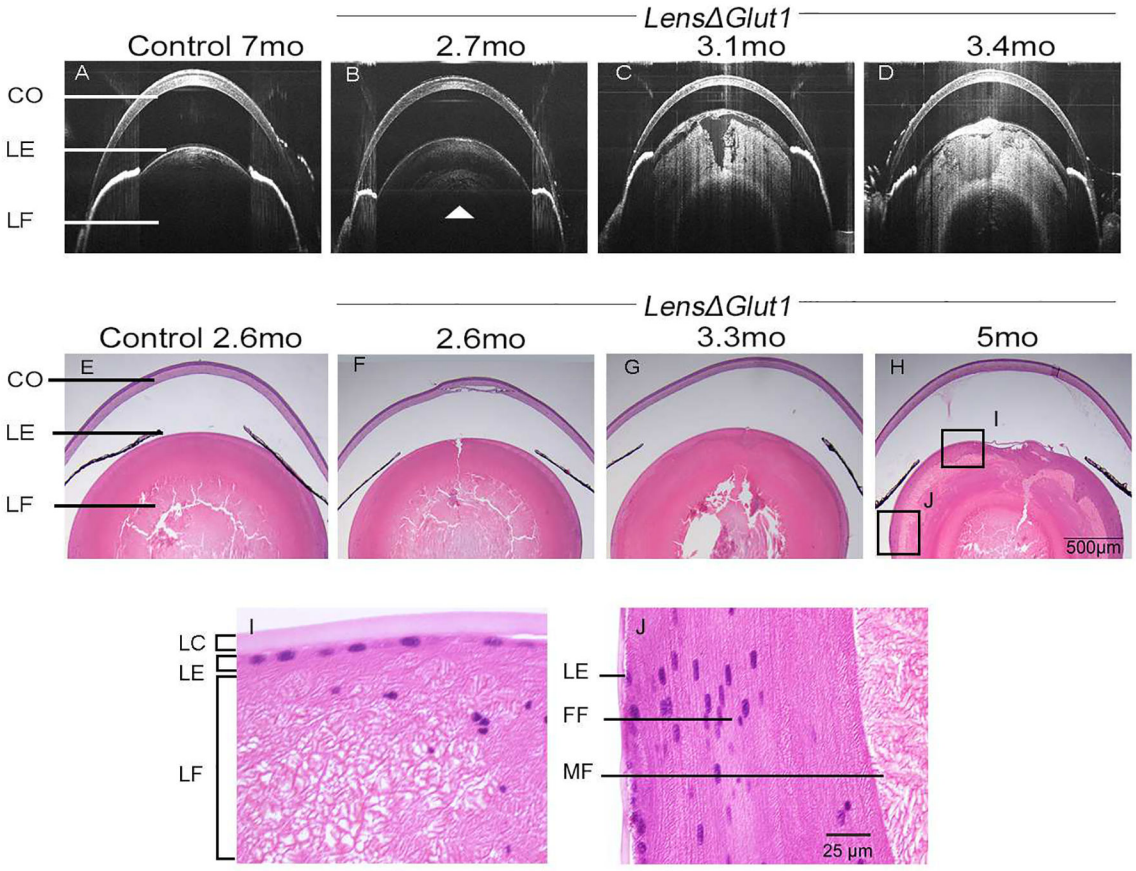

Figure 4: Age-related progression of *LensΔGlut1* cataracts

SD-OCT images of a control *GFAP-Cre*$^{+/0}$ mouse at 7 months (**A**) and of a representative *LensΔGlut1* mouse imaged at three ages: 2.7 months (**B**), 3.1 months (**C**) and 3.4 months (**D**). In 4B, the white arrow shows a nuclear cataract forming at 2.7 months. Comparison of 4B, 4C, 4D illustrates increasing cataract severity with increasing age. H&E stained paraffin sections of eyes from control *GFAP-Cre*$^{+/0}$ mouse at 2.6 months (E) and from *LensΔGlut1* mice at ages 2.6 months (F), 3.3 months (G) and 5 months (H). The morphology of the *LensΔGlut1* lens deteriorates with age. Higher power images of *LensΔGlut1* mouse lens at 5 months (I and J). Lens fiber cells are disorganized in both the anterior (I) and equatorial (J) regions of the *LensΔGlut1* mouse. CO: Cornea, LE: Lens epithelium, LC: Lens capsule, LF: Lens fiber cells, FF: Forming fiber cells, MF: Mature fiber cells

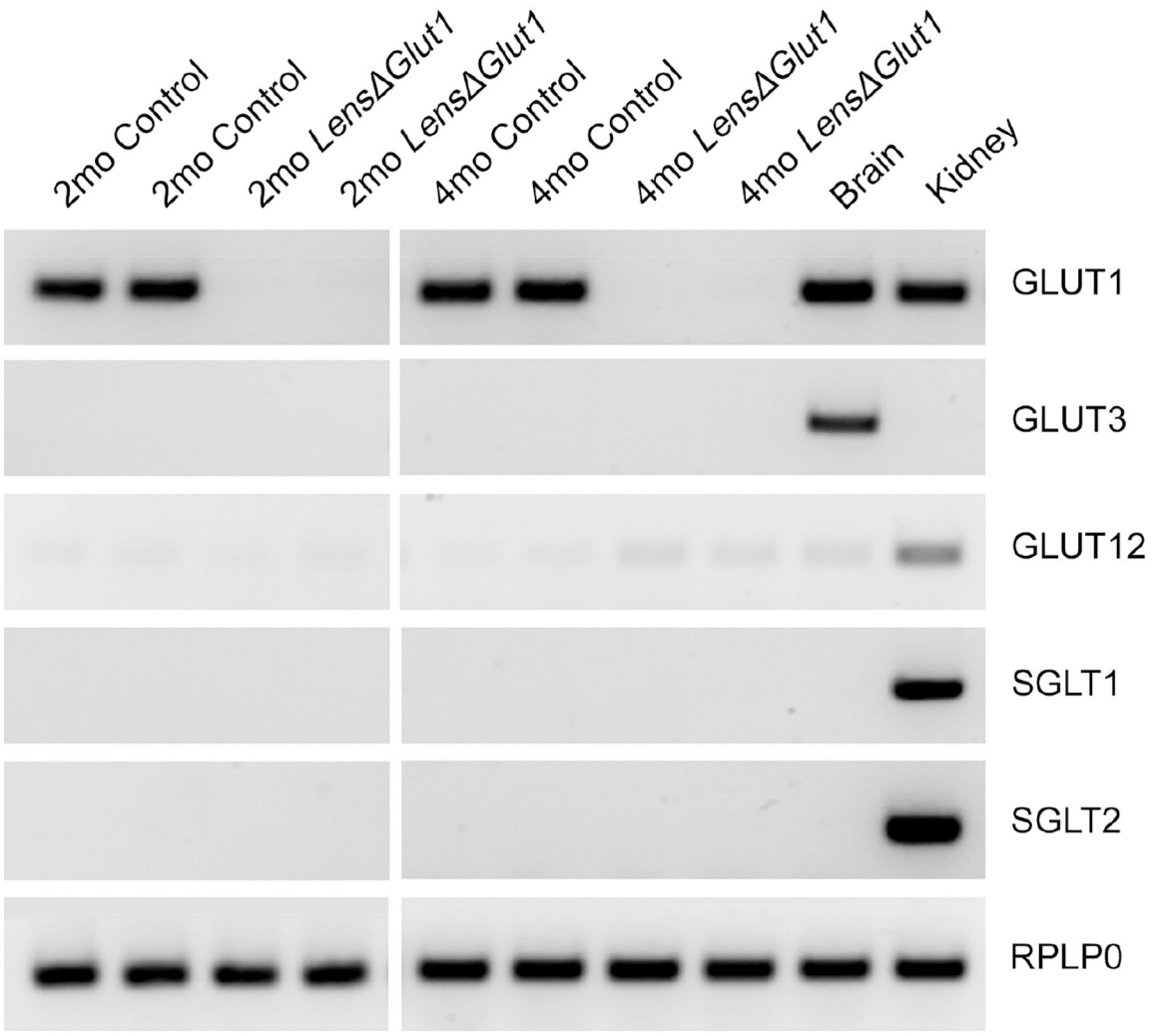

Figure 5: In the absence of GLUT1, there was no compensation from other glucose transporters

Reverse images of sybrgreen-stained amplicons after 30 cycles of PCR amplification with primers specific for glucose transporter family members using cDNA prepared from whole lenses of 2-month-old and 4-month-old control and *LensΔGlut1* mice. cDNA prepared from brain and kidney were used as positive controls. RPLP0 primers were used as an internal control.

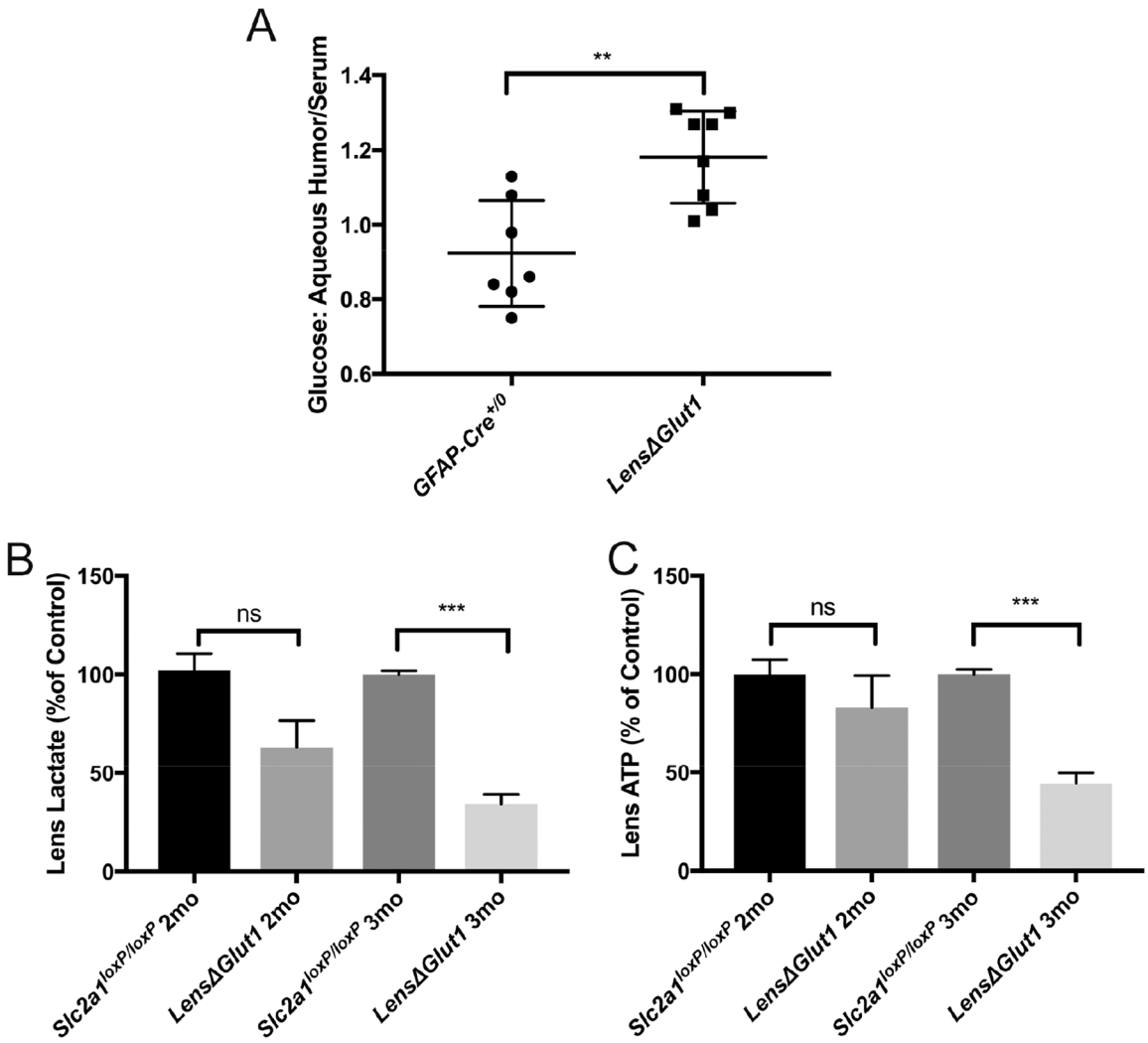

Figure 6: Deletion of GLUT1 from the lens epithelium results in increased levels of glucose in the aqueous humor and decreased levels of ATP and lactate in the lens.

A. The ratio of glucose concentration in the aqueous humor to that in the blood was significantly higher in *LensΔGlut1* mice (n=7) relative to *GFAP-Cre*$^{+/0}$ mice (n=8). In the lens, levels of lactate (**B)** and ATP (**C)** were reduced in *LensΔGlut1* mice (n=6) relative to *Slc2a1*$^{loxP/loxP}$ mice (n=6). These reductions were significant at 3 months of age, but not at 2 months.

Table 1:

List of primers used for RT-PCR

Primer Name	Forward	Reverse	PCR Product
Slc2a1	GGCCTGACTACTGGCTTTGT	TGCATTGCCCATGATGGAGT	150bp
Slc2a3	GGTGGAGCGGTGAAGATCAG	GAGATGGGGTCACCTTCGTT	287bp
Slc2a12	GGAGCTAG CAAAG GCGAA	GACTGTCCCCTTCCACACAG	144bp
Slc5a1	GGATCAGGTCATTGTGCAGC	TGGTGTGCCGCAGTATTTCT	196bp
Slc5a2	GGTGGAGCGGTGAAGATCAG	GAGATGGGGTCACCTTCGTT	287bp
RPLP0	AGATTCGGGATATGCTGTTGGC	TCGGGTCCTAGACCAGTGTTC	109bp

Table 2:

GC-MS analysis of amino acids in the aqueous humor of *LensΔGlut1* mice compared to control. Data was expressed as percentage change in the amino acid levels *LensΔGlut1* mice (n=3) to control mice (n=3).

Amino Acid	Percent Change	Standard Error
Aspartate	88.57%	28.63
Lysine	75.73%	12.53
Threonine	60.97%	33.89
Glutamate	43.13%	20.14
Serine	38.73%	28.39
Alanine	32.08%	4.76
Asparagine	19.61%	9.74
Glutamine	9.11%	7.10
Glycine	6.84%	8.19
Tryptophan	4.06%	7.78
Valine	−7.40%	3.25
Isoleucine	−7.50%	4.93
Beta-Alanine	−7.84%	3.17
Methionine	−18.87%	11.56
Leucine	−20.11%	4.62
Histidine	−23.44%	5.28
N-Asp	−27.84%	13.27
Phenylalanine	−53.75%	17.37
Tyrosine	−61.09%	11.72